

A molecular mechanism for sensory adaptation based on ligand-induced receptor modification

(methylation/phosphorylation/densitization/adenylate cyclase/chemotaxis)

BARRY E. KNOX*, PETER N. DEVREOTES*, ALBERT GOLDBETER†, AND LEE A. SEGEL‡

*Department of Biological Chemistry, Johns Hopkins University, School of Medicine, Baltimore, MD 21205; †Faculte des Sciences, Universite Libre de Bruxelles, CP 231, B-1050 Brussels, Belgium; and ‡Department of Applied Mathematics, The Weizmann Institute of Science, 76100 Rehovot, Israel

Communicated by J. T. Bonner, December 12, 1985

ABSTRACT Physiological responses mediated by cell-surface receptors frequently adapt or "desensitize" (i.e., terminate despite persistent occupancy of receptors by ligand). Binding of ligands to the external domains of a wide variety of surface receptors induces covalent modification of their cytoplasmic domains. A mechanism is presented in which the variety of receptor states generated by ligand binding and covalent modification act together to regulate physiological responsiveness. The development of the model is guided by observations of adaptation for chemotaxis in *Escherichia coli* and adenylylase activation in *Dictyostelium*. The general features of the marked response and eventual exact adaptation predicted by the model match those observed in the experimental systems.

Physiological responses mediated by cell-surface receptors are said to adapt or "desensitize" if they terminate despite persistent occupancy of receptors by ligand. Adaptation can be viewed as a reversible adjustment of cell sensitivity to the level of the stimulus. In systems that adapt, there is an attenuation of the response in the presence of a constant prolonged stimulus; no further response is detected as long as the stimulus is held constant. Recovery of sensitivity (deadaptation or "resensitization") begins when the stimulus is removed. However, additional responses can be elicited without the need for a recovery period, if the level of receptor occupancy is directly increased. In this case, the magnitude of each serial response is determined by the change in receptor occupancy (1-11).

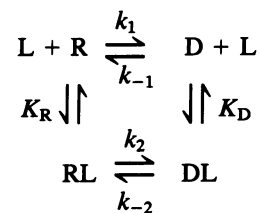
Binding of ligand to the external domain of a wide variety of surface receptors induces reversible covalent modification of their cytoplasmic domains (12-19). In a number of systems, the kinetics and concentration dependence of ligand-induced receptor phosphorylation is closely correlated with adaptation of the receptor-mediated physiological response (20, 21). In bacteria, attractant-induced carboxymethylation is necessary for adaptation of the chemotactic response (12, 22, 23). In such cases, it is natural to assume that adaptation occurs because the modification shifts the receptor from an "active" to an "inactive" state. This simple assumption is insufficient to account even for the basic experimental observations. For instance, a small stimulus will induce modification of only a small fraction of the receptors. Nevertheless, the elicited response will terminate. Thus, the response subsides even though most of the receptors remain in the unmodified or "active" state. To explain this discrepancy and others, we have sought a simple theoretical treatment that would unite the experimental observations of receptor modification and sensory adaptation.

We describe here a conceptual framework for viewing response and adaptation in terms of receptor modification. We first explore the kinetics of receptor modification and

illustrate a simple experiment that can be performed to measure modification and demodification rate constants *in vivo*. We then propose a novel mechanism in which the variety of receptor states generated by ligand binding and modification act together to regulate physiological responsiveness. The scheme depends only on the dissociation constants for ligand binding, the rate constants for receptor modification and demodification, and the basal and total activity. Once these are determined, there are no free parameters. The model accounts for the general features that have been observed in studies of receptor-mediated adaptation. It describes systems that adapt exactly as well as those that only partially adapt. Our formulation, which directly links receptor modification to the control of adaptation, displays all of the properties of earlier phenomenological schemes but is a specific molecular implementation.

KINETICS OF RECEPTOR MODIFICATION

As shown in the reaction scheme below, we begin with the assumption that the free receptor can be found in two states, R and D, where D is a covalently modified form of R. Addition of a ligand, L, brings about the formation of two occupied forms, RL and DL. Interconversion by reversible covalent modification takes place between RL and DL as well as between R and D. The ligand binding steps are assumed to be fast compared to the rates of modification and demodification. This assumption allows determination of the fraction of receptor in each of the four states as a function of time.



Prior to the addition of stimulus, an equilibrium between R and D exists that is determined by k_1 and k_{-1} . The addition of a saturating ligand concentration leads eventually to a new equilibrium determined by k_2 and k_{-2} . Since the extent of receptor modification is experimentally accessible, we display kinetic changes through graphs of the fraction of modified receptor. The expression for the fraction of modified receptor is $([D] + [DL])/R_T$ where R_T is the total amount of receptor. Fig. 1 A and B show the time course of receptor modification and subsequent demodification, which occurs upon addition and removal of a saturating stimulus. Addition of a stimulus that occupies only 50% of the receptors leads to a lower steady-state level of receptor modification, and a further increment in receptor modification results when the stimulus is increased to saturation. The legend to Fig. 1

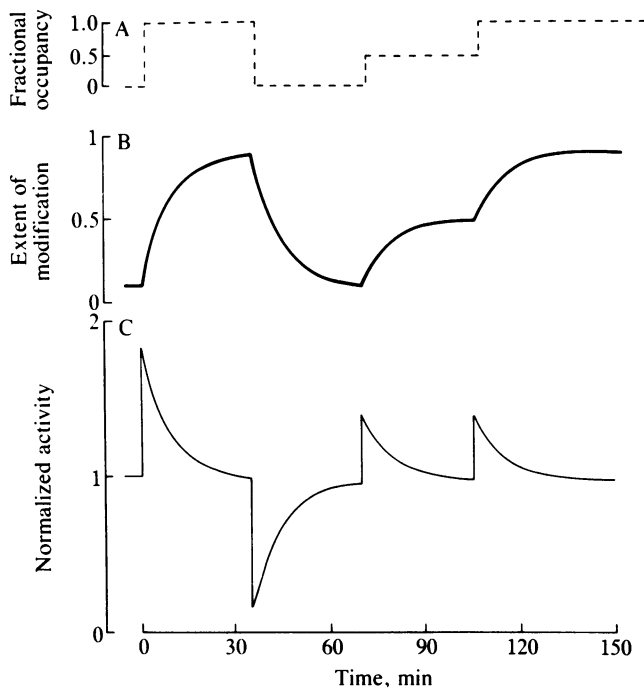


FIG. 1. (A and B) Kinetics of changes in the fraction of modified receptors elicited by sudden changes in ligand concentration. (A) Dashed line in panel A indicates the addition and removal of ligand plotted as fractional occupancy, $[L]/(K_D + [L])$. The ligand was raised from 0 to $100 K_D$. After 35 min it was removed. After an additional 35 min, the ligand concentration was raised from 0 to K_D . After 35 min it was further increased from K_D to $100 K_D$. Solid line in B shows kinetic changes in the fraction of modified receptors, $([D] + [DL])/R_T$. When it is possible to obtain experimental data for the extent of receptor modification, $([D] + [DL])/R_T$, by using a protocol similar to that shown in A and B, the rate constants can be calculated. When $[L] = 0$, the fraction of modified receptor equals $[D]/([D] + [R])$, since there are no liganded receptor forms, and $[R]/[D] = k_{-1}/k_1$. ($[R]/[D] = 10$ in this example.) When $[L]$ is increased to $100 K_D$, there are only liganded receptor forms, RL and DL, and the half-time for the increase in the fraction of modified receptors is given by $\ln 2/(k_2 + k_{-2})$. ($t_{1/2} = 6.3$ min in this example.) Once an equilibrium between RL and DL is attained, the fraction of modified receptors equals $[DL]/([DL] + [RL])$ and $[RL]/[DL] = k_{-2}/k_2$. ($[RL]/[DL] = 1/10$ in this example.) When $[L]$ is decreased to 0, the half-time for the decrease in the fraction of modified receptors is given by $\ln 2/(k_1 + k_{-1})$. ($t_{1/2} = 6.3$ min in this example.) Thus, the experiment shown in the left-hand portion of A and B gives experimental data values for four equations in four unknowns, which completely determines the rate constants. Rate constants calculated from the extent of modification given in this example are: $k_1 = 0.01 \text{ min}^{-1}$, $k_{-1} = 0.1 \text{ min}^{-1}$, $k_2 = 0.1 \text{ min}^{-1}$, and $k_{-2} = 0.01 \text{ min}^{-1}$ and $K_D = K_R$. (C) Kinetics of changes in activity elicited by sudden changes in ligand concentration: corresponding changes in normalized activity [activity (A) divided by basal activity, A_0]. Activity changes in all figures are normalized in this manner. The values of the weights used in C ($a_1 = 0.11$; $a_2 = 0.20$; $a_3 = 0.09$) were calculated from the rate constants according to the formulae: $(a_1 - A_0/R_T)/k_1 = (a_2 - A_0/R_T)/k_2 = -(a_3 - A_0/R_T)/k_{-2} = -(a_4 - A_0/R_T)/k_{-1}$. In this case, A_0/R_T and a_4 were chosen equal to k_{-1} and 0, respectively. In individual systems, the basal activity can be experimentally determined, and the total observed activity can be used to determine a_4 .

outlines how one can obtain the interconversion rate constants k_1 , k_{-1} , k_2 , and k_{-2} from experimental data. Fig. 2A shows the extent of modification as a function of ligand concentration. The steady-state extent of modification increases with ligand concentration and saturates. The half-maximal extent of modification occurs at the dissociation constant for binding.

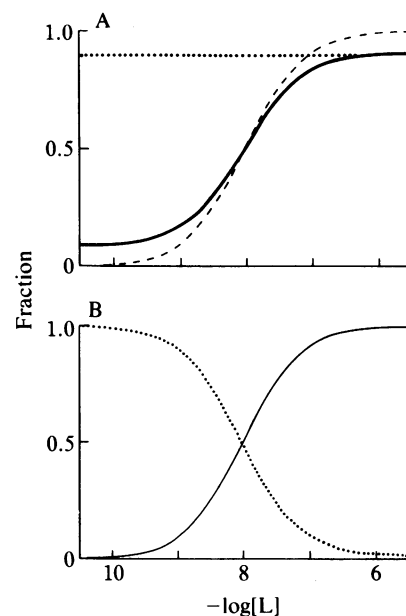


FIG. 2. (A) Predicted concentration dependence of the extent of receptor modification. —, Steady-state fraction of modified receptor $([D] + [DL])/R_T$ as a function of ligand concentration; ..., final steady-state fraction of modified receptor following a step from the indicated ligand concentration to a saturating ligand concentration; ---, receptor occupancy. (B) Predicted concentration dependence of integrated activity. —, Integrated activity (sum of activity for each time point) for a step from 0 to each indicated ligand concentration;, integrated activity for a step from each indicated ligand concentration to a saturating concentration. Rate constants for this figure are the same as those for Fig. 1. K_D was chosen as 10^{-8} M.

ADAPTATION BASED ON RECEPTOR MODIFICATION

How can receptor modification bring about exact adaptation? Our fundamental assumption is that all states of the receptor contribute to the generation of the physiological response. For instance, consider that each of the receptor states binds an effector molecule with a different affinity constant and that the response depends on the relative amount of bound effector. When the total amount of effector is constant, changes in the amount of bound effector depend only on changes in the distribution of receptors among the four receptor states. The quantity that expresses the changes in receptor contribution to the response we define as activity. Specifically, the activity is given by a weighted sum of the four forms of the receptor:

$$\text{activity} = a_1[R] + a_2[RL] + a_3[DL] + a_4[D]$$

The "weights" a_1 , a_2 , a_3 , and a_4 are constants that give the relative contributions of each receptor state to the total activity. In the above example, the weights are the affinity constants of each receptor state for the effector molecule. In cases where receptors couple to the response by controlling enzyme activities or ion channels, the activity will have the same mathematical form, but the weights will have corresponding biochemical interpretations. Thus, it is sufficient to examine activity to understand how receptor modification controls the response.

We have demonstrated that changes in ligand concentration elicit transient changes in activity. The mathematical documentation of this result is presented elsewhere (24). We have made the interesting finding that exact adaptation occurs when each of the weights is related to the lifetime of its receptor state. That is, the system will adapt exactly when the shortest lived receptor states are weighted most heavily.

Note that the weights are not chosen arbitrarily but are determined by the rate constants of receptor modification and demodification. Once the rate constants are experimentally determined, there are no free parameters in this formulation.

Fig. 1C shows the activity changes corresponding to the receptor modification changes discussed for Fig. 1A and B. To emphasize changes in activity, all values have been normalized to activity prior to application of the stimulus (i.e., basal activity), which can be experimentally determined for each system. Note that we have assumed for simplicity that the initial activity changes triggered by stimulus addition or removal reflect changes in fractional occupancy, which equilibrates instantaneously. The saturating stimulus leads to a large activity that returns to the prestimulus level. Removal of the ligand generates subbasal activity, which again returns to the prestimulus level. Application of two successive increments in ligand concentration leads to two corresponding increases in activity, which each return to the basal state. For the parameters used, the sum of the integrated activities generated by the two stimuli equals the integrated activity generated by the single increment to the highest ligand concentration.

Fig. 2B indicates relationships between binding and integrated activity. There is an increase in the amount of integrated activity obtained on raising the stimulus level from zero to the indicated concentration of ligand (solid line). When the stimulus is subsequently increased to a saturating level, the additional integrated activity elicited by the second increment in stimulus decreases to zero (dotted line). The extent of modification attained after the second increment reaches the same final steady-state level in all cases (Fig. 2A). Thus, it is seen that the additivity relationship depicted in Fig. 1 in fact holds for any set of serial increments in ligand concentration.

Figs. 1 and 2 have been drawn for the "symmetric" case wherein $(k_1 + k_{-1})$ equals $(k_2 + k_{-2})$ and K_D equals K_R . In this case, as shown in Fig. 1, the half-times for adaptation and deadaptation are equal. The concentrations of L yielding both half-maximal extent of modification and half-maximal activity coincide with the dissociation constant for binding, $K_R = K_D$. When $(k_1 + k_{-1})$ is found to be larger than $(k_2 + k_{-2})$, then the model predicts that adaptation is slower than deadaptation, and the coincident curves for both extent of modification and integrated activity will be shifted to the right of the binding curve. When $(k_1 + k_{-1})$ is smaller than $(k_2 + k_{-2})$, then adaptation is predicted to be faster than deadaptation, and the modification and activity curves should be shifted to the left of the binding curve. Note that when $(k_1 + k_{-1})$ is not equal to $(k_2 + k_{-2})$, the additivity relationships shown in Fig. 1 do not hold. Also, if $K_D \neq K_R$, then the steady-state curves will not be Michaelian.

The model accounts for other phenomena often observed in sensory systems—for example, deadaptation. This is shown in Fig. 3A–C, which depict the effect of two identical stimuli separated by a variable recovery interval (see Fig. 3A *Inset*). The activity elicited by the second stimulus progressively increases with recovery time until it reaches the level generated by the first stimulus. The half-time of deadaptation is independent of the magnitude of the paired stimuli.

Fig. 3D–F shows a method to estimate the rate of adaptation. Responses to test stimuli are measured after various durations of pretreatment by a higher stimulus (see Fig. 3D *Inset*). The magnitude of the activity generated by the test stimulus decreases as the duration of pretreatment is increased. When the duration of pretreatment exceeds a certain characteristic time, the response to the test stimulus vanishes. At this characteristic time, the higher stimulus has already produced the level of adaptation that eventually would be engendered by the test stimulus. For a given pretreatment stimulus, the characteristic time increases as

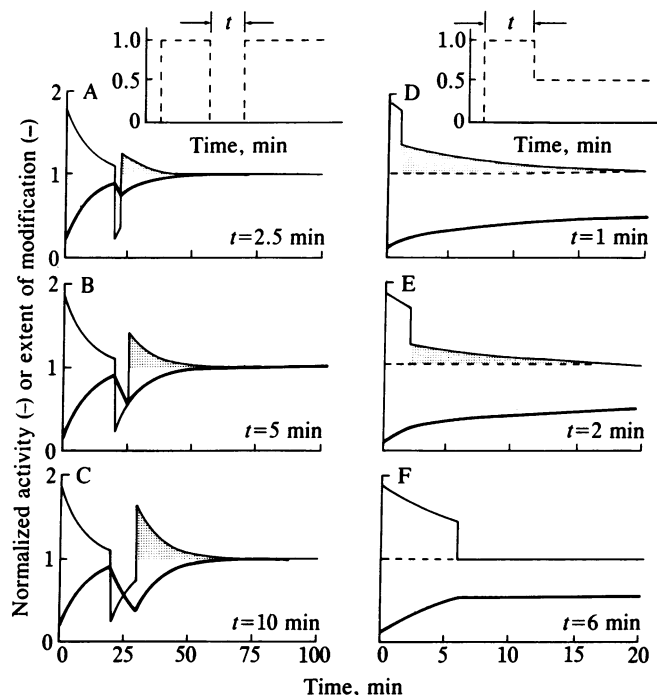


FIG. 3. Adaptation and deadaptation properties. (Left) Stimulus protocol to measure deadaptation rate. Two successive saturating stimuli were applied, separated by a variable "recovery time," t (see A *Inset*). The initial stimulus was 20 min in duration. A–C show the effect of increasing recovery time. Activity changes elicited by the second stimulus are indicated by the shaded curves. (Right) Stimulus protocol to measure the rate of adaptation. Ligand concentration is increased from 0 to $100 K_D$, the pretreatment stimulus. After a pretreatment time interval, t , the concentration is lowered directly to K_D , the test stimulus, with no interposed recovery period (see D *Inset*). D–F show the effect of increasing pretreatment times. Activity changes elicited by the test stimulus are indicated by the shaded curves. —, Activity; ---, basal activity for reference; —, extent of receptor modification. Rate constants and weights are the same as those used in Fig. 1.

the concentration of the test stimulus increases. This gives an estimate of the rate of adaptation as a function of stimulus level.

The fact that the receptor-mediated activity adapts exactly to all increments (regardless of the stimulus) in ligand concentration is remarkable, given that the distribution between the four receptor states depends strongly on ligand concentration. Fig. 4A illustrates the steady-state contribution of each of the four receptor states to the total activity as a function of ligand concentration. It is seen that, although each individual contribution varies strongly with the ligand concentration, the four contributions always add up to the same activity. Nevertheless, Fig. 4B shows that upon the addition of ligand, the activity that is initially elicited is significantly above basal. Roughly speaking, the reason that this occurs is that, upon addition of ligand, heavily weighted receptor forms predominate and a significant activity ensues. Exact adaptation occurs for all ligand concentrations because of a redistribution of the amount of receptor in each of the four states. The amount of activity contributed by each of the states again adds up to the basal activity.

COMPARISON WITH EXPERIMENTAL DATA

To test this model, we have examined data for two well-studied sensory systems, those responsible for chemotaxis in *E. coli* and *Salmonella* and cAMP secretion in *Dictyostelium*. In bacteria, chemoattractants trigger "smooth swimming"

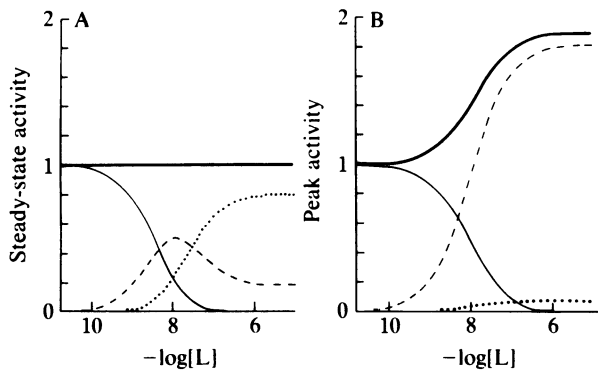


FIG. 4. Contribution of individual receptor states to activity. Graphs show the contribution of each of the four receptor states to activity. (A) Activity either before or an infinite time after a step increment from 0 to the indicated ligand concentration. (B) Activity immediately after stimulus application. —, Contribution of R, $a_1[R]$; ---, contribution of RL, $a_2[RL]$;, contribution of DL, $a_3[DL]$ (in this example, a_4 is 0, and there is no contribution of D); —·—·, the sum of the four contributions, which is defined as activity. Rate constants and weights were the same as those used in Fig. 1.

responses. Adaptation of this response requires carboxymethylation of the chemoreceptors (12, 22, 23). In *Dictyostelium*, extracellular cAMP leads to activation of adenylate cyclase. Adaptation of this response is closely correlated with modification of surface cAMP receptors detected as an electrophoretic mobility shift, likely due to phosphorylation (16, 21). Fig. 5 A and B shows receptor modification data in each system for a saturating step increase and later removal of the stimulus (16, 25). The four rate constants, k_1 , k_{-1} , k_2 , and k_{-2} for interconversion of the receptor states were calculated for each set of data by using the procedure outlined in the legend of Fig. 1. The solid lines

represent the amount of modified receptor predicted by the model using these rate constants. As indicated in the legend to Fig. 1, the rate constants fix the values of the weights.

The activity in each system, predicted by the model, using these weights is shown in Fig. 5 C and D. For comparison, the observed biological responses are shown in Fig. 5 E and F. After addition of the stimulus, the predicted activity matches the observed response in both systems. The predicted activity returns to basal at the same time that the biological responses adapt. According to the model, removing the ligand leads to a drop in activity below basal. In the bacteria, this is reflected in an increased tumbling frequency (1). In *Dictyostelium*, such a subbasal activity has not yet been observed. There is also good agreement between experiment and theory for recovery experiments of the type illustrated in Fig. 3A. Both the rapid recovery time observed in bacteria and the gradual recovery that is characteristic of *Dictyostelium* are accounted for by the model (1, 2, 5).

DISCUSSION

We have presented a conceptual framework for understanding in molecular terms how receptor modification can govern sensing and adaptation. It was assumed that, in the presence of ligand, the receptor existed in four different states, each of which contributed, with a certain weight, to an activity. It was shown that there exists a set of weights such that the system responds to stimulus and then exactly adapts. A method was presented to derive from experimental data on receptor modification the various rate and dissociation constants and to use these constants to determine the weights. Although no free parameters remain, most of the major behaviors of cellular sensory systems are accounted for by the model. In particular, data for reversible modification of chemoreceptors in bacteria or surface cAMP receptors in *Dictyostelium* were analyzed to obtain rate constants. These

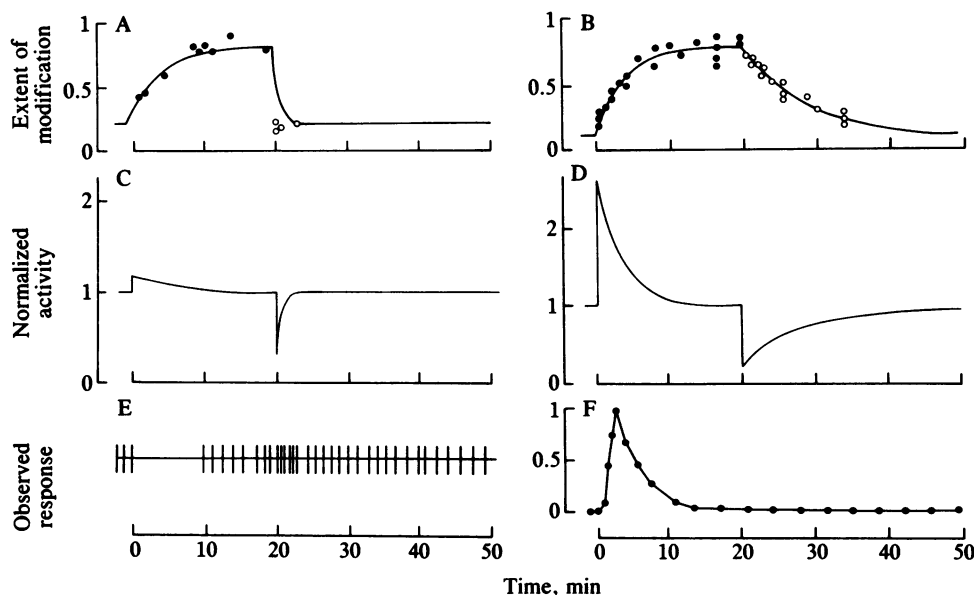


FIG. 5. Comparison of the model with experimental data for chemotaxis in *E. coli* (Left) and cAMP-induced cAMP secretion in *Dictyostelium* (Right). Shown are kinetic changes after a 0–100 K_D step increase in stimulus, followed by removal at 20 min. (A and B) Data for the extent of methylation of methylated chemotaxis proteins in *E. coli* or the fraction of modified cAMP receptors in *Dictyostelium* (16, 25). ●, Increase in the extent of modification after addition of stimulus; ○, decrease in the extent of modification after removal of stimulus. For *E. coli* it was assumed that the initial and final extents of modification were 0.2 and 0.8, respectively. Data were analyzed as described in Fig. 1 to obtain rate constants k_1 , k_{-1} , k_2 , and k_{-2} . These constants ($k_1 = 0.276$, $k_{-1} = 1.104$, $k_2 = 0.182$, and $k_{-2} = 0.046$ for *E. coli* and $k_1 = 0.012$, $k_{-1} = 0.104$, $k_2 = 0.22$, and $k_{-2} = 0.055$ for *Dictyostelium*) were used for all simulations in this figure. Solid lines passing through data were drawn by the model. (C and D) Predicted activity changes in each system. (E and F) Response observed in each system. In *E. coli* (E), a response is measured in terms of tumble frequency. Tumbles are indicated as vertical ticks on the horizontal time axis (25). In *Dictyostelium* (F), response is indicated as the rate of secretion of [3H]cAMP (●), which is plotted on a normalized scale (16).

rate constants were used to calculate the weights for each system. By using these weights, activity changes were generated that had similar kinetics to the corresponding physiological responses. Correlation between theory and experiment has been obtained for such features as dose-dependence, relationships between extent of modification and extent of activity, additivity of responses, deadadaptation, and relationships between rates of adaptation and deadadaptation.

Our framework also may apply to other sensory systems. For example, both the β -adrenergic receptor of turkey erythrocytes and rhodopsin in the rod outer segment show ligand-induced phosphorylation, which is correlated with adaptation of the respective physiological responses. The present results also may be useful in assigning a role to receptor modification where the function of such modification remains unknown. It may turn out that, when a sensory system is carefully examined, it does not adapt exactly. The model can account for partial adaptation, but here the weights are calculated from the rate constants by slightly different formulas than those presented in Fig. 1. The major predictions of the model are preserved.

The major assumption of our scheme is that the variety of receptor states act together to generate an activity. How does the activity regulate physiological responsiveness? To provide one answer, let us examine the example mentioned above in which the activity coefficients, a_1 , a_2 , a_3 , and a_4 , represent affinity constants for binding an effector molecule to each of the receptor forms. There is increasing evidence that transducing proteins, such as guanyl-nucleotide binding proteins G_s , G_i , and transducin and perhaps some of the *che* gene products in *E. coli*, are activated by direct binding to receptors. On stimulation, the balance of receptor types alters, and an increased amount of effector is bound to receptors. This binding interaction elicits the physiological response. Detailed analysis of this notion led to several interesting points. The ratio of the number of effector molecules to receptors determines the gain of the response system. At ratios larger than 1, small changes in activity bring about large increases in response. The ratio also can determine the kinetics of the response. When the ratio is small, the kinetics of the response resembles that of activity. However, when the ratio is greater than 1, saturation effects begin to appear. When the stimulus is added, a maximal response is observed until activity drops below a given level. Thus, under these conditions, the duration of the response rather than the magnitude depends on the dose of the applied stimulus. In fact, dose-dependent response duration is observed for the chemotactic response in bacteria (2, 3). Similar analyses can be carried out in systems where the response is coupled via enzyme activities or ion channels, but the weights would be interpreted as enzyme turnover numbers or probabilities of channel opening.

Previously, two general classes of models have been proposed for sensory adaptation. One type defines phenomenological parameters that govern the behavior of the system (1, 26, 27). The "adapting box" described here provides a detailed molecular implementation for these models. A second type of model is based specifically on receptor modification (28–32). These models can be shown to be special cases of the "adapting box" wherein only one or a few receptor states are assumed to be active or activity is defined in a less tangible way.

Our framework suggests an approach to the study of sensory systems. When it is known that receptors are

covalently modified, then the single experiment shown in Fig. 1 gives the rate constants and hence the weights. Then simulations can be carried out to determine whether the observed behavior is as predicted and to suggest further experiments. When little is known about receptor modification, as in the case of leukocyte chemotaxis, one can still challenge our model by measuring rates of physiological adaptation and deadadaptation, which lead to specific predictions of the relationship of the dose–response curve to the binding curve.

This work was supported by Public Health Service Grant GM 28007 to P.N.D., who is an American Heart Association Established Investigator.

1. Macnab, R. M. & Koshland, D. E., Jr. (1972) *Proc. Natl. Acad. Sci. USA* **69**, 2509–2512.
2. Spudich, J. L. & Koshland, D. E., Jr. (1975) *Proc. Natl. Acad. Sci. USA* **72**, 710–713.
3. Berg, H. C. & Tedesco, P. M. (1975) *Proc. Natl. Acad. Sci. USA* **72**, 3235–3239.
4. Devreotes, P. & Steck, T. (1979) *J. Cell Biol.* **82**, 300–309.
5. Dinauer, M., Steck, T. & Devreotes, P. (1980) *J. Cell Biol.* **86**, 545–553.
6. Dinauer, M., Steck, T. & Devreotes, P. (1980) *J. Cell Biol.* **86**, 554–561.
7. Harden, T., Su, Y. & Perkins, J. (1979) *J. Cyclic Nucleotide Res.* **5**, 99–106.
8. Su, Y.-F., Harden, T. & Perkins, J. (1980) *J. Biol. Chem.* **55**, 7410–7419.
9. Zigmond, S. & Sullivan, S. (1979) *J. Cell Biol.* **82**, 517–527.
10. Matthews, G. & Baylor, D. (1981) *Curr. Top. Membr. Transp.* **15**, 3–18.
11. Hudspeth, A. (1983) *Ann. Rev. Neurosci.* **6**, 187–216.
12. Goy, M. F., Springer, M. S. & Adler, J. (1977) *Proc. Natl. Acad. Sci. USA* **74**, 4964–4968.
13. Stadel, J., Nambi, P., Lavin, T., Heald, S., Caron, M. & Lefkowitz, R. (1982) *J. Biol. Chem.* **257**, 9242–9245.
14. Klein, C., Lubs-Haukeness, J. & Simons, S. (1985) *J. Cell Biol.* **100**, 715–720.
15. Klein, P., Theibert, A., Fontana, D. & Devreotes, P. (1984) *J. Biol. Chem.* **259**, 1757–1764.
16. Devreotes, P. & Sherring, J. (1985) *J. Biol. Chem.* **260**, 6378–6383.
17. Kasuga, M., Karlsson, F. & Kahn, C. (1982) *Science* **215**, 185–187.
18. Buhrow, S., Cohen, S., Garbers, D. & Staros, J. (1983) *J. Biol. Chem.* **258**, 7824–7827.
19. Wilden, U. & Kuhn, H. (1982) *Biochemistry* **21**, 3014–3022.
20. Stadel, J., Nambi, P., Shorr, R., Sawyer, D., Caron, M. & Lefkowitz, R. (1983) *Proc. Natl. Acad. Sci. USA* **80**, 3173–3177.
21. Klein, P., Fontana, F., Knox, B., Theibert, A. & Devreotes, P. (1985) *Cold Spring Harbor Symp. Quant. Biol.* **50**.
22. Parkinson, J. & Revello, P. (1978) *Cell* **15**, 1221–1230.
23. Russo, A. & Koshland, D. (1983) *Science* **220**, 1016–1020.
24. Segel, L., Goldbeter, A., Devreotes, P. & Knox, B. (1986) *J. Theor. Biol.*, in press.
25. Springer, M., Goy, M. & Adler, J. (1979) *Nature (London)* **280**, 279–284.
26. Delbruck, M. & Reichardt, W. (1956) in *Cellular Mechanisms in Differentiation and Growth*, ed. Rudnick, D. (Princeton University Press, Princeton, NJ), pp. 3–44.
27. Koshland, D. (1977) *Science* **196**, 1055–1063.
28. Katz, B. & Thesleff, S. (1957) *J. Physiol.* **138**, 63–80.
29. Goldbeter, A. & Koshland, D. (1982) *J. Mol. Biol.* **161**, 395–416.
30. Martiel, J. & Goldbeter, A. (1984) *C. R. Hebd. Seances Acad. Sci. Ser. C* **298**, 549–552.
31. Swillens, S. & Dumont, J. (1977) *J. Cyclic Nucleotide Res.* **97**, 173–177.
32. Block, S., Segall, J. & Berg, H. (1983) *J. Bacteriol.* **154**, 312–323.